Ruthenium(Platinum)-Doped Tin Dioxide Inverted Opals for Gas Sensors: Synthesis, Electron Paramagnetic Resonance, Mössbauer, and Electrical Investigation

M. Acciarri,[†] R. Barberini,[†] C. Canevali,[†] M. Mattoni,[†] C. M. Mari,[†] F. Morazzoni,*[,†] L. Nodari,[‡] S. Polizzi,[§] R. Ruffo,[†] U. Russo,[‡] M. Sala,[†] and R. Scotti[†]

Dipartimento di Scienza dei Materiali, INSTM, Università di Milano-Bicocca, Via R.Cozzi 53, 20125 Milano, Italy, Dipartimento di Scienze Chimiche, Università degli Studi di Padova, Via Marzolo 1, 35131 Padova, Italy, and Dipartimento di Chimica Fisica, INSTM, Università di Venezia, Via Torino 155, 30172 Venezia, Italy

Received July 28, 2005. Revised Manuscript Received September 26, 2005

Tin dioxide and ruthenium(platinum)-doped tin dioxide were synthesized in the form of inverted opals, aiming to investigate the interaction of these materials with CO reducing gas. The results of electron paramagnetic resonance (EPR) investigation allowed us to conclude that CO interaction causes the formation of singly ionized oxygen vacancies located in the subsurface region. These ones transfer their electrons to transition metal centers, Ru or Pt, enhancing the SnO_2 surface reactivity toward CO. The reduction of Ru^{4+} and Pt^{4+} was assessed both by EPR and Mössbauer spectroscopy. Resistance measurements showed that the materials are well-suitable for use in CO sensor devices because of their reproducible and fast electrical response; this was related to the homogeneous and high dispersion of Ru and Pt centers in the oxide matrix and to the subsurface location of the species active in the electron-transfer processes.

Introduction

Transition metal (Ru,Pt)-doped nanocrystalline SnO_2 obtained by sol−gel procedure provided highly sensitive materials to be used in semiconductor gas sensors. Their peculiar morphological properties allowed us to investigate the gas-sensing mechanism by spectroscopic and spectromagnetic measurements in great depth.[1−6] In fact, the particle size of these semiconductor materials ranged between 3 and 6 nm; this resulted in a high surface/volume ratio and enhanced the surface reactivity, enabling us to detect the intermediate species active at the solid−gas interface, both in powders and thin films. Electron paramagnetic resonance (EPR) was demonstrated to be the technique of choice for revealing oxide defects (singly ionized oxygen vacancies $V_o^{\bullet}$) and chemisorbed oxygen species (superoxide anion O_2^-), both related to the resistance variations of SnO_2 under CO(NO) gas interaction. We already demonstrated[1−6] that the changes in the electrical response S ($S = R_{air}/R_{gas}$) between undoped and transition metal-doped (Ru,Pt) SnO_2, under CO(NO) treatment, depend on the following equilibria:

$$O_o + CO \leftrightarrows CO_2 + V_o \quad (1)$$

$$V_o \leftrightarrows V_o^{\bullet} + e^- \quad (2)$$

(O_o is the oxide anion in a regular oxygen site, V_o is the neutral oxygen vacancy, and $V_o^{\bullet}$ the singly ionized oxygen vacancy.)

$$Ru(Pt)^{4+} + nV_o^{\bullet} \leftrightarrows Ru(Pt)^{(4-n)+} + nV_o^{\bullet\bullet} \quad (3)$$

($V_o^{\bullet\bullet}$ is the doubly ionized oxygen vacancy, $n = 1$ for Ru, $n = 2, 4$ for Pt.)

The electron transfer of reaction (3) right-hand-shifts the equilibria of reactions (1) and (2), increasing the number of V_o defects and of electrons injected into the conduction band, with respect to undoped SnO_2. It was suggested[6] that this enhances the electrical response of the transition metal-doped SnO_2 with respect to the undoped oxide.

In the past few years a number of ceramics[7] were prepared as ordered architectures of opal and inverted opal. Among them SnO_2 inverted opal, a material built by nanocrystalline bridges and junctions around a regular arrangement of air spheres, was reported to display theoretical ideal gas sensing

* To whom correspondence should be addressed.
[†] Università di Milano-Bicocca.
[‡] Università degli Studi di Padova.
[§] Università di Venezia.

(1) Canevali, C.; Chiodini, N.; Di Nola, P.; Morazzoni, F.; Scotti, R.; Bianchi, C. M. *J. Mater. Chem.* **1997**, *7*, 997−1002.
(2) Morazzoni, F.; Canevali, C.; Chiodini, N.; Mari, C. M.; Ruffo, R; Scotti, R.; Armelao, L.; Tondello, E.; Depero, L. E.; Bontempi, E. *Chem. Mater*. **2001**, *13*, 4355−4361.
(3) Acciarri, M.; Canevali, C.; Mari, C. M.; Mattoni, M.; Ruffo, R.; Scotti, R.; Morazzoni, F.; Barreca, D.; Armelao, L.; Tondello, E.; Bontempi, E.; Depero, L. E. *Chem. Mater*. **2003**, *15*, 2646−2650.
(4) Armelao, L.; Barreca, D.; Bontempi, E.; Morazzoni, F.; Canevali, C.; Depero, L. E.; Mari, C. M; Ruffo, R.; Scotti, R.; Tondello, E. *Appl. Magn. Reson*. **2002**, *22*, 89−100.
(5) Canevali, C.; Mari, C. M.; Mattoni, M.; Morazzoni, F.; Scotti, R.; Ruffo, R; Russo, U.; Nodari, L. *Sens. Actuators B* **2004**, *100*, 228−235.
(6) Canevali, C.; Mari, C. M.; Mattoni, M.; Morazzoni, F.; Nodari, L.; Russo, U.; Ruffo, R; Scotti, R. *J. Phys. Chem. B* **2005**, *109*, 7195−7202.
(7) Xia, Y.; Gates, B.; Yin, Y.; Lu, Y. *Adv. Mater.* **2000**, *12*, 693−713.

10.1021/cm051670c CCC: $30.25
Published on Web 11/03/2005

behavior.[8] However, no attempt was done up to now to enhance the electrical response of SnO_2 inverted opal by doping the pure oxide with transition metals, and no spectroscopic investigation was reported that rationalizes the structure−function relationship in such a morphology of materials.

The present paper is concerned with the preparation of SnO_2 and ruthenium (platinum)-doped SnO_2 as inverted opals. The interaction of CO with either pure and transition metal-doped tin dioxide was studied by EPR, Mössbauer, and electrical resistance measurements, to understand the structure−function relationships in the periodic macroporous materials, compared with those of nanostructured powders and thin films.[2−6,9]

Experimental Section

Reactants. The colloidal suspensions of polystyrene latex microspheres (ca. 200 nm diameter) in water (2.5 wt %) were from Alfa Aesar.

Tetrakis(*tert*-butoxy)tin(IV), [$Sn(OBu^t)_4$], was prepared according to the literature.[10] Tris(acetylacetonate)ruthenium(III), [$Ru(acac)_3$], and bis(acetylacetonate)platinum(II), [$Pt(acac)_2$], were Aldrich pure chemicals.

Pure (argon, oxygen, air) and mixed [CO(600 ppm)/argon and CO(800 ppm/air)] gases were purchased from SAPIO.

The organic vehicle used to prepare samples for the electrical measurements was ESL 413 Thinner, kindly supplied by ESL Europe.

Preparation of Undoped and Ru(Pt)-Doped SnO_2 Inverted Opals. Polystyrene opal was first prepared by centrifugating (3 h, 2000 rpm) the colloidal aqueous suspension of microspheres. After removal of the solvent, the opal was dried at 308 K for 24 h, then placed in a vial, and further dried in vacuo (10^{-1} Torr) at room temperature for 30−60 min.

Undoped inverted opal SnO_2 was obtained by dropwise impregnation of the polystyrene template under a dry N_2 atmosphere with a solution of [$Sn(OBu^t)_4$] in anhydrous ethanol (360 mg/cm^3), at variance with the procedure in ref 8 that uses pure melted tin *tert*-butoxide. After impregnation, the solvent was removed under vacuum (10^{-1} Torr) at room temperature for 30 min, and then the sample was kept under a moist nitrogen atmosphere (100% relative humidity) for about 3−4 h. Finally, the sample was heated at 723 K in flowing O_2 (30 cm^3/min) for 10 h, using a three steps temperature ramp (30 min at 373, 473, and 573 K).

Ru(Pt)-doped SnO_2 inverted opals were prepared by impregnating the polystyrene template with a solution of [$Sn(OBu^t)_4$], [$Ru(acac)_3$], or [$Pt(acac)_2$], having Ru(Pt):Sn 8×10^{-3} molar ratio in the minimum amount of anhydrous ethanol. The subsequent steps of the procedure were common with the undoped oxide.

Microstructural Investigation. The sample morphology was analyzed by scanning electron microscopy (SEM) using a Vega TS5136 XM Tescan microscope in a high-vacuum configuration. The electron beam excitation was 30 kV at a beam current of 25 pA and the working distance was 12 mm. In this configuration the beam spot was 38 nm. Previous to the SEM analysis, samples were gold-sputtered.

High-resolution transmission electron microscopy (HRTEM) analyses were performed at 300 kV using a JEOL 3010 apparatus with a high-resolution pole piece (0.17 nm point-to-point resolution), equipped with a Gatan slow-scan 794 CCD camera. Elemental composition was determined by an Oxford Instruments EDS microanalysis detector (Mod. 6636). Samples were ground in an agate mortar and the resulting fine powder was suspended in 2-propanol. A 5 μL drop of this suspension was deposited on a holey carbon film supported on a 3 mm copper grid for TEM investigation.

Electron Paramagnetic Resonance (EPR) Measurements. EPR spectra were recorded on powdered samples by a conventional Bruker EMX spectrometer operating at the X band frequency and with magnetic field modulation of 100 kHz, with microwave power of 10 and 5 mW and modulation amplitude of 10 and 3 G. The g values were calculated by comparison with diphenylpicryl-hydrazyl (DPPH) standard sample ($g = 2.0036$).The amounts of paramagnetic species were calculated by double integration of the resonance line area, taking as reference the area of the Bruker weak pitch ($9.7 \times 10^{12} \pm 5\%$ spin cm^{-1}) in the case of $V_o^{\bullet}$ centers, and the area of the [$Ru(acac)_3$]−SnO_2 xerogel sample ($g_{\parallel} = 1.55$, $g_{\perp} = 2.14$ with Ru/Sn 0.008 molar ratio),[9] in the case of Ru^{3+} centers.

Powdered samples were put into a quartz apparatus suitable for both gas flow interaction and EPR measurements. After each thermal gas treatment, the samples were quenched at room temperature (in about 5 min) and EPR spectra were recorded at 123 K, under the same atmosphere. When oxygen is present, the spectra were recorded under an argon atmosphere, to avoid line broadening due to the possible interaction between molecular oxygen and paramagnetic surface oxygen species.

The following sequence of treatments was adopted:

(i) Ru(Pt)SnO_2 samples were conditioned in a dry air stream (30 cm^3 min^{-1}) for 1 h at 673 K (samples Ru^1673 and Pt^1673).

(ii) CO (600 ppm)/argon mixture was passed over samples $Ru^1(Pt^1)673$ (30 cm^3 min^{-1}) at the indicated temperature T(K) and the contact was maintained for 30 min (samples Ru^2T and Pt^2T). The T values were 298, 373, 473, 573, and 673 K.

(iii) Then samples $Ru^2(Pt\ ^2)T$ were exposed to a dry air stream (30 cm^3 min^{-1}) at room temperature for 10 min (samples $Ru^3(Pt^3)$-298.

The same sequence of treatments was performed on undoped inverted opal SnO_2 and the samples were indicated $Sn^{1(2,3)}T$.

Mössbauer Measurements. Mössbauer experiments on selected samples, having undergone treatments as indicated in EPR measurements, were performed at 80.0 K. The source, $Ca^{119m}SnO_3$, nominal strength 15 mCi, New England Nuclear Corporation, was at room temperature and moved with constant acceleration, giving a triangular waveform. Suitable computer programs were employed in the fitting procedure of the experimental spectra to Lorentzian line shapes by using least-squares minimization techniques. The isomer shift data are relative to room-temperature $CaSnO_3$. Samples were prepared by finely grinding about 10.0 mg of powder and mixing with vaseline. The suspension was inserted into a lead container and placed inside the cryostat. All the manipulations were carried out in a glovebox under a nitrogen atmosphere.

Electrical Measurements. Pastes were obtained by mixing the inverted opal powders with the organic thinner in a 1:1 w:w ratio, and then thick films of about 400 μm were deposed by the Doctor Blade method onto SiO_2 insulating substrate, thermally grown on a Si wafer. Samples were dried at 773 K for 4 h in flowing oxygen, to completely remove the organics.

Two gold electrodes (10 mm × 4 mm) were deposited at a distance of about 2 mm from each other onto the oxide film by the dc sputtering technique. The samples were put in a quartz chamber

(8) Scott, R. W. J.; Yang, S. M.; Chabanis, G.; Coombs, N.; Williams, D. E.; Ozin, G. A. *Adv. Mater.* **2001**, *13*, 1468−1472.
(9) Canevali, C.; Chiodini, N.; Morazzoni, F.; Scotti, R. *J. Mater. Chem.* **2000**, *10*, 773−778.
(10) Hampden-Smith, M. J.; Wark, T. A.; Rheingold, A.; Huffman, J. C. *Can. J. Chem.* **1991**, *69*, 121−129.

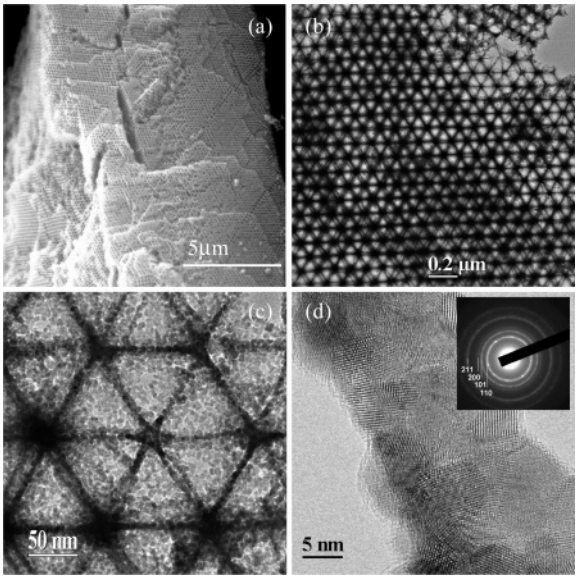

Figure 1. (a) SEM, (b), (c) TEM, and (d) HRTEM micrographs of Ru-doped SnO_2 inverted opals. In the inset the selected-area electron diffraction pattern matches well with intensities and indexes of the SnO_2 structure.

and placed in an oven and the measurements were performed at different temperatures, ranging from 298 to 673 K. The electrical resistance was measured by a Keithley 617 programmable electrometer and the data acquisition was controlled by the PC.

The following sequence of treatments was adopted:

The sensing element was equilibrated in air flow (30 $cm^3\ min^{-1}$) at the selected temperature, and then CO (800 ppm)/air mixture was introduced (30 $cm^3\ min^{-1}$) up to equilibrium conditions. The starting resistance conditions of the film were restored by air equilibration, before introducing again the CO/Ar mixture. *S* is the electrical response defined as the ratio between the film resistance under flowing air, R_{air}, and that under flowing CO/air mixture, R_{gas}, respectively.

Results and Discussion

Both undoped and transition metal-doped materials consist of bridges and junctions of nanocrystalline cassiterite particles (average size 5−8 nm) surrounding a regular structure of hollow spheres (ca. 160 nm diameter, a value 20% lower that of the template spheres). The SEM picture shows the large extension and homogeneity of the samples grown (Figure 1a).

TEM and HRTEM analyses confirmed that no morphological modifications were derived from the doping by transition metals. No crystalline phases other than cassiterite were detected. The morphologies of the Ru-doped SnO_2 inverted opals are shown in Figure 1 as an example.

Energy dispersive X-ray (EDX) analysis, carried out in the TEM, was able to detect the small peaks of the ruthenium L and K-lines and of the platinum L and M-lines. Although a quantitative determination of the Ru(Pt):Sn ratio is not warranted, the height of peaks attributed to Ru and Pt were fairly constant on different points of the samples, suggesting a good dispersion homogeneity.

The electron spin resonance spectra of Sn^1673, recorded at 123 K under an argon atmosphere, gave well-detectable resonance lines at $g = 1.896$. These were unequivocally assigned[1] to singly ionized oxygen vacancies $V_o^{\bullet}$. The amount

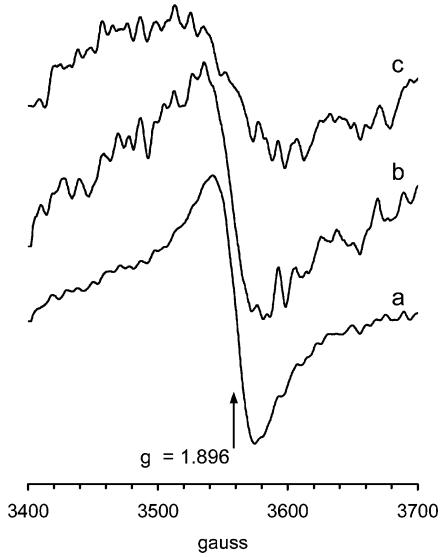

Figure 2. EPR spectrum of SnO_2 inverted opals samples: (a) Sn^1673; (b) Sn^2473; (c) Sn^2673.

of these defects in Sn^1673 was 10^{16} spin/g. It did not show very relevant modifications in intensity, under CO/Ar treatment at different temperatures, Sn^2T. However, the increase of temperature caused a well-detectable line broadening, specially at 673 K (Figure 2); thus, it may be thought that the $V_o^{\bullet}$ amount really increased, but spin−spin interaction masked the effect on the resonance line area.

The exposure to air stream, Sn^3T(K), had no effect on the resonance lines. It appears that, at variance with the nanosized sol−gel obtained SnO_2 powders,[1] the singly ionized oxygen defects, in inverted opal SnO_2, do not undergo the reaction

$$V_o^{\bullet} + Sn_{Sn} + O_2 \leftrightarrows V_o^{\bullet\bullet} + Sn_{Sn}{-}O_2^{-} \qquad (4)$$

They are unable to transfer their electrons to O_2 at room temperature and to produce the paramagnetic superoxide anion. This indicates that, not being sensitive to the O_2 interaction, the oxygen defects are located in a subsurface region. The lack of the surface reactivity towards oxygen at room temperature also suggests that the surface damage, induced by the interaction with the reducing gas, undergoes very fast self-repair and surface reconstruction of the inverted opals ordered architecture as compared to the disordered nanosized materials.[1]

The oxygen defects fully diffuse toward the bulk; thus, at variance with the sol−gel prepared conventional powders, all EPR detectable defects become active donors injecting electrons into the conduction band.

Ru^1673 and Pt^1673 did not evidence any EPR resonance, in line with the electron transfer of reaction (3) and with the behavior of nanosized powders and thin films.[2,6,9]

After CO/Ar treatment Ru^2T(K) samples showed the resonance lines of magnetically diluted Ru^{3+} centers (Figure 3). $V_o^{\bullet}$ signals were still absent. The resonances attributable to transition metal centers became well-visible from 573 K and were identical to those observed in nanocrystalline Ru-doped SnO_2.[6,9] By analogy with that reported in ref 9, signals were attributed to the sum of three single species having

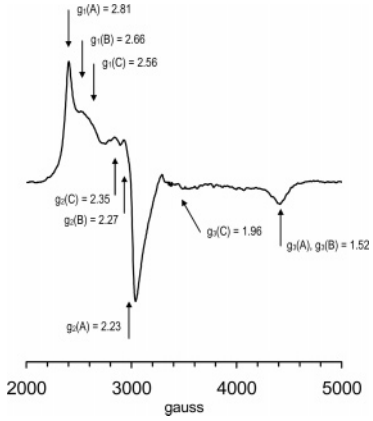

Figure 3. EPR spectrum of Ru^2673 (spectrum obtained by accumulating 50 scans).

Ru^{3+} centers in different symmetry fields of oxide anions[11,12] and already identified by simulation and fitting of the spectra:[9] Ru^{3+}(A) ($g_1 = 2.81$, $g_2 = 2.23$, $g_3 = 1.52$), Ru^{3+}(B) ($g_1 = 2.66$, $g_2 = 2.27$, $g_3 = 1.52$), and Ru^{3+}(C) ($g_1 = 2.56$, $g_2 = 2.35$, $g_3 = 1.96$). The number of paramagnetic Ru^{3+} centers was calculated from the integrated area of the whole spectrum, by taking as reference area that of a $[Ru(acac)_3]-SnO_2$ xerogel sample (before annealing at 723 K) with Ru:Sn 0.008 molar ratio (see Experimental Section). The Ru^{3+} amount increased with the CO/Ar temperature and at 673 K it corresponded to about that of the nominal doping metal.

Ru^{3+} centers oxidized again after reaction with oxygen at 673 K, but were unable to be reoxidized at RT following

$$Ru^{3+} + O_2 + Sn^{4+} \leftrightarrows Sn^{4+} - O_2^- + Ru^{4+} \qquad (5)$$

Also this behavior disagrees with that reported for nanosized[6,9] Ru-doped SnO_2, suggesting that all Ru^{3+} centers, as already $V_o^\bullet$ centers, lie in the subsurface region in inverted opal materials. Even in the presence of transition metal centers, the templated oxide did not lose its strong tendency to repair the surface damaged by CO, revealing an unexpected shape memory.

Pt-doped SnO_2 inverted opal did not show EPR resonances, under any gas treatment. Unfortunately, the absence and/or the too low surface amount of platinum centers hindered the use of photoelectron spectroscopy (XPS) to investigate the Pt electronic state.

To obtain further insight into the effects of Ru- and Pt-doping centers, in particular the EPR silent Pt centers, Mössbauer investigation of Sn centers was carried out. Table 1 reports the related parameters.

The Mössbauer spectra of Sn^1673, Ru^1673, and Pt^1673 showed the presence of a single absorption around zero velocity. The absorptions were all well-fitted by symmetrical quadrupole split doublets, having parameters typical of inorganic tin(IV) compounds. The same was found for CO-(600 ppm)/Ar treated pure oxide, Sn^2673. Instead in the case of Ru(Pt)-doped SnO_2 any attempt to fit the spectra as either a single line or a paramagnetic doublet failed, due to the presence of a small residual absorption at positive velocity. The spectra were thus fitted, obtaining in every case good χ^2 values, to two strongly overlapped symmetrical quadrupole split doublets, both with parameters typical of inorganic tin(IV) compounds. It must be stressed that the parameters are affected by large errors, due to the strong overlap.

Table 1. Mössbauer Parameters for SnO_2 and Ru(Pt)-Doped SnO_2 Inverted Opal Powders at 80.0 K

	δ (mm/s)	ΔE_Q (mm/s)	Γ (mm/s)	area %	total area (mm/s/mg)
Sn^1673	0.19(1)	0.47(5)	1.25(6)		0.004118
Sn^2673	0.18(1)	0.52(2)	0.98(3)		0.004229
Pt^1673	0.20(1)	0.56(3)	1.09(5)		0.004693
Pt^2673	0.22(1)	0.41(7)	1.11(6)	70	0.009195
	0.19(5)	1.43(9)	1.07(8)	30	
Ru^1673	0.22(1)	0.60(3)	1.07(4)		0.001115
Ru^2673	0.18(1)	0.57(7)	1.18(6)	60	0.003157
	0.18(3)	1.76(7)	1.26(9)	40	

The first more intense doublet is attributable to Sn centers very similar to those of undoped SnO_2; the second, lower in intensity, showed an electron density at the nucleus similar to the previous one, but a more distorted electronic distribution specially in the case of Ru doping. This may be associated with the presence of reduced metal centers that modify the electron symmetry of the nearer tin centers. In no case absorptions due to tin(II) species (for SnO $\delta = 2.74$, ΔE_Q 1.93 mm/s) were detected,[13] at variance with what was previously reported in the literature.[14]

The results described in the present paper suggest that the electron injected by CO, at 673 K, are transferred toward transition metal centers, according to reaction (3). In Ru-doped samples the electron transfer was both assessed by EPR direct analysis and deduced from the Sn electronic distortion (Mössbauer), while in Pt-doped samples the reduction became evident only from the Mössbauer data.

It may be interesting to underline the behavior of the resonant absorption area (see Table 1) among the various samples. In fact, the area remains virtually constant for the samples Sn^1673 and Sn^2673 and Pt^1673, while the addition of Ru, sample Ru^1673, causes a strong area decrease, as if the metal doping affects the strength of the Sn−O bonds, without influencing the tin electron density. This may suggest different bonding interactions of Pt and Ru with the surrounding lattice oxide anions (stronger for Ru−O than for Pt−O). Moreover, the treatment with CO in Ru(Pt)-doped materials is responsible for the increase of the resonant area, suggesting that the reduction of Ru^{4+} and Pt^{4+} to Ru^{3+} and $Pt^{(4-n)+}$($n = 2, 4$) decreases the interaction between Ru(Pt) and oxide anions and increases the strength of the Sn−O lattice bond.

To investigate in depth the structure−function relationship of the SnO_2 inverted opals for gas-sensing materials, the electrical response S was measured in samples prepared by the same powders used for the spectromagnetic analyses.

The results are collected in Figure 4, where two pulses at 673 K were also reported for all types of samples. No significant difference in the response of SnO_2 and Ru(Pt)−

(11) Carl, P. J.; Larsen, S. C. *J. Catal.* **2000**, *196*, 352−361.
(12) Chaudhary, V. A.; Mulla, I. S.; Vijayamohanan, K.; Hegde, S. G.; Srinivas, D. *J. Phys. Chem. B* **2001**, *105*, 2565−2571.
(13) Geenwood. N. N.; Gibb. T. C. *Mossbauer Spectroscopy*; Chapman & Hall: London, 1971.
(14) Sofonova, O.; Bezwerkhy, I.; Fabrichnyi, P.; Rumyantseva, M.; Gaskov, A. *J. Mater. Chem.* **2002**, *12*, 1174−1178.

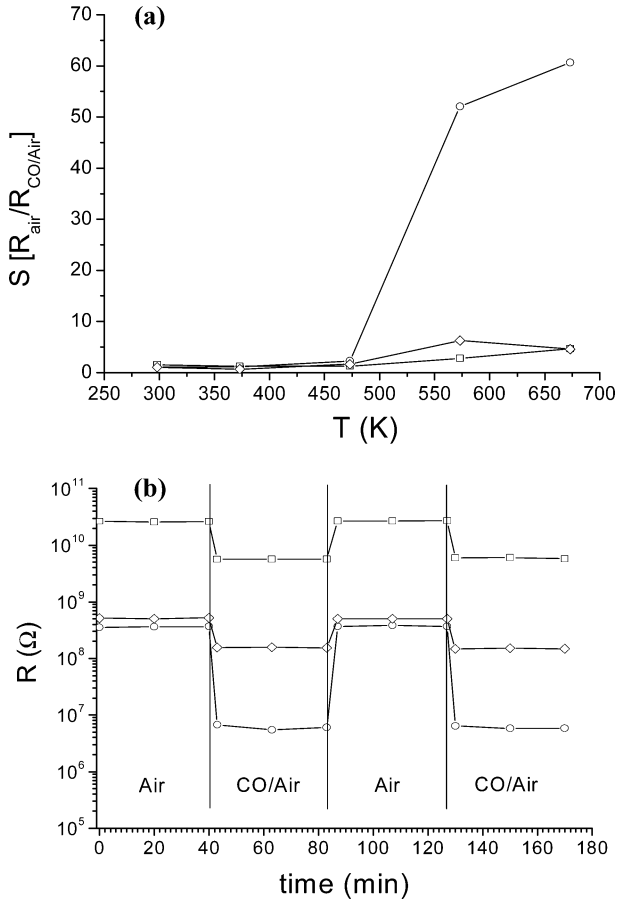

Figure 4. (a) Plot of the electrical sensitivity *S* vs *T* (K) for (□) SnO_2, (◇) Ru-doped SnO_2, and (○) Pt-doped SnO_2. (b) Resistance variation under two subsequent pulses alternating air to CO(800 ppm)/air. Symbols are the same as in (a).

SnO_2 was observed until 473 K; the values slowly increase with the temperature. Above 473 K, Pt-doped specimens presented a paramount increase in *S* values with respect to pure SnO_2 and Ru−SnO_2; in particular, at 573 and 673 K the electrical response of Pt−SnO_2 resulted in 52 and 62, respectively, while the other samples showed values around 5. Such a behavior agrees well with that observed in the case of sol−gel obtained films[2,3] and with the increase of electrical response generally observed in Pt-doped SnO_2.[15,16]

The reproducibility and the fast responses suggest this type of film is suitable for sensing devices.

Although it may be arduous to relate the results of measurements taken in different conditions, like EPR spectra performed at 123 K and electrical measurements performed in the range 298−673 K, it could be suggested that the broadening of $V_o^{\bullet}$ lines seen in $Sn^2$673 was probably due to the increase of singly ionized oxygen vacancies, each other magnetically interacting. This is related to the maximum *S* value at 673 K.

Conclusions

Spectromagnetic and electrical investigation of undoped and Ru(Pt)-doped SnO_2, in the form of inverted opal, evidence the following:

(i) The macroporous ordered SnO_2 solid reacts with CO, forming oxygen defects at the surface, not differently from the corresponding nanosized powder;[1] instead the inverted opal surface shows a stronger tendency to repair the damage (V_0 defects) by migration of the subsurface oxygen atoms from their regular sites. This is probably a consequence of the very high surface:volume ratio that prompts fast surface rebuilding. The subsurface final position of the oxygen defects induces their shallow location in the semiconductor energy gap and their easy ionization.

(ii) The results of the spectromagnetic investigations reported here for SnO_2-based inverted opal materials, both undoped and Ru(Pt)-doped, definitely confirm the main conclusion of our previous investigations,[1−6] that the change of electrical response consequent to CO interaction is mediated by the oxygen defects. The electron transfer from $V_o^{\bullet}$ to transition metal centers (reaction (3)), demonstrated by EPR in Ru-doped SnO_2 and by Mössbauer in Pt-doped SnO_2, is thus responsible for the right-hand shifts of reactions (1) and (2.) This enhances the electrical response.

(iii) The electrical response of SnO_2-based inverted opal materials is not quantitatively different from that of the nanosized materials.[4] However, all inverted opal materials, both undoped and transition metal-doped, show fast and well-reproducible responses. This behavior is possibly related to the fact that the electron exchange with the conduction band mainly involves bulk sites, unaffected by surface variations.

CM051670C

(15) Esfandyarpour, B.; Mohajerzadeh, S.; Famini, S.; Khodadadi, A.; Asl Soleimani, E. *Sens. Actuators B* **2004**, *100*, 190−194.

(16) Mandayo, G. G.; Castao, E.; Gracia, F. J.; Cirera, A.; Cornet, A.; Morante, J. R. *Sens. Actuators B* **2003**, *95*, 90−96.